

Inhibition of corrosion processes on copper in aerated sodium chloride solutions by 5-(3-aminophenyl)-tetrazole

El-Sayed M. Sherif · R. M. Erasmus ·
J. D. Comins

Received: 11 March 2008 / Accepted: 11 July 2008 / Published online: 19 August 2008
© Springer Science+Business Media B.V. 2008

Abstract Inhibition of corrosion processes of copper in aerated 3.5% NaCl solutions by 5-(3-aminophenyl)-tetrazole (APT) has been investigated using open-circuit potential, potentiodynamic polarization, potentiostatic current–time, electrochemical impedance spectroscopy, and weight loss measurements together with pH and Raman spectroscopy. Increasing concentrations of APT greatly decreased the corrosion rate and increased the surface and polarization resistance. It was concluded that the adsorption of APT blocks the active sites on the copper surface leading to the formation of cuprous chloride and oxychloride complexes. This was supported by the Raman spectrum obtained from the copper surface after 24 days of immersion in a 3.5% NaCl solution containing 5.0 mM APT. The results collectively are in good agreement and show clearly that APT is a good corrosion inhibitor for copper under the conditions studied.

Keywords 5-(3-Aminophenyl)-tetrazole · Copper corrosion inhibition · Electrochemical techniques · Raman spectroscopy · Sodium chloride solution

El-Sayed M. Sherif is on leave from Physical Chemistry Department, National Research Centre, Dokki, Cairo, Egypt.

E.-S. M. Sherif (✉) · R. M. Erasmus · J. D. Comins
DST/NRF Centre of Excellence in Strong Materials,
Physics Building, University of the Witwatersrand,
Johannesburg,
Wits 2050, South Africa
e-mail: Elsayed.sherif@wits.ac.za

R. M. Erasmus · J. D. Comins
Raman and Luminescence Laboratory, School of Physics,
University of the Witwatersrand, Johannesburg, Wits 2050,
South Africa

1 Introduction

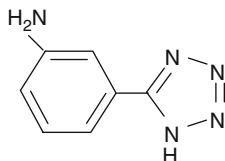
In applications such as pipelines for water utilities, heat conductors, heat exchangers, etc., copper is often corroded by being in contact with sea water.

In previous work, the corrosion reactions of copper [1] were reported, while the effects of organic additives on corrosion inhibition of both copper [2–10] and aluminum [11, 12] were studied in different corrosive environments. A variety of electrochemical and gravimetric techniques were used, together with surface characterization methods such as XPS, AES, SEM, EDX, FT-IR, UV-vis and Raman spectroscopy.

In spite of the relatively noble potential of copper, corrosion takes place at a significant rate in sea water and other chloride environments [2–4, 13, 14]. Heterocyclic compounds, especially nitrogen-based ones, are effective inhibitors, being coordinate with Cu(0), Cu(I) or Cu(II) via their nitrogen atoms through lone pair electrons to form polymeric complexes with copper [3, 5, 15–17]. These form an adsorbed protective film on the copper surface, providing inhibition of corrosion by acting as a barrier to aggressive ions such as chloride [16–19]. Polar functional groups such as nitrogen, sulfur, and oxygen and conjugated double bonds are considered reaction centers in establishing the adsorption process [8, 9, 20–22].

The present study reports the inhibition of copper corrosion in 3.5% NaCl solutions by the heterocyclic azole compound 5-(3-aminophenyl)-tetrazole (APT, Scheme 1) whose effects on the corrosion inhibition of metals and alloys in corrosive media have not been reported previously. It was anticipated that APT would be effective in the present case since it contains four nitrogen groups besides the aminophenyl group whose presence increases the ability of the nitrogen groups to be adsorbed onto the copper surface.

Scheme 1 5-(3-Aminophenyl)-tetrazole (APT)



2 Experimental procedure

2.1 Chemicals and electrochemical cell

APT (Alfa-Aesar, 96%), sodium chloride (NaCl, Merck, 99%), and absolute ethanol (C₂H₅OH, Merck, 99.9%) were used as received. An electrochemical cell with a three-electrode configuration was used; a copper rod (Cu, Goodfellow, 99.999%, 0.5 cm in diameter), a platinum foil, and an Ag/AgCl electrode (in saturated KCl) were used as a working, counter, and reference electrodes, respectively. The copper electrodes were first polished successively with metallographic emery paper of increasing fineness of up to 800 grits, washed with distilled water, degreased with acetone, washed with distilled water again, and finally dried using tissue paper.

2.2 Electrochemical methods

Electrochemical experiments were performed by using a PARC Parstat-2273 Advanced Electrochemical System after immersion periods 1 and 24 h of the copper electrode in the test electrolyte. For potentiodynamic polarization experiments the potential was scanned from -800 to 700 mV at a scan rate of 1 mV/s. Potentiostatic current-time experiments were carried out by stepping the potential at 250 mV for 120 min. Electrochemical impedance spectroscopy (EIS) tests were performed at corrosion potentials (E_{Corr}) over a frequency range of 100 kHz– 0.05 Hz, with an ac wave of ± 5 mV peak-to-peak overlaid on a dc bias potential, and the impedance data were collected using Powersine software at a rate of 10 points per decade change in frequency.

2.3 Gravimetric method

Measurements consisted in recording a change in the mass of copper specimens (Goodfellow, 99.999%) as a result of spontaneous dissolution in chloride solutions in the absence and presence of APT. The experiments were carried out using rectangular copper coupons having the dimensions of 3.0 cm in length, 1.0 cm in width and 0.20 cm in thickness with an exposed total area of 7.6 cm². The coupons were polished and dried as for the case of copper rods (see Sect. 2.1), weighed (W_1), and then suspended in 200 cm³ of the test solutions for different exposure periods (6 – 24 days).

After the designated exposure, the specimens were rinsed with distilled water, washed with acetone to remove a film possibly formed due to the inhibitor, dried using tissue paper, and weighed again (W_2). Three specimens were used for each test and the loss in weight was calculated by taking an average of these values. The maximum standard deviation in the observed weight loss was calculated to be $\pm 1.0\%$. The weight loss (Δm , mg dm⁻²), the corrosion rate (R_{Corr} , mg dm⁻² day⁻¹ (mdd)), the inhibition efficiency (IE%), and the degree of surface coverage (θ) over the exposure time were calculated as follows [6, 7],

$$\Delta m = \frac{W_1 - W_2}{A}, \quad (1)$$

$$R_{\text{Corr}} = \frac{W_1 - W_2}{At}, \quad (2)$$

$$\text{IE}\% = \frac{R_{\text{Corr}}^{\text{un}} - R_{\text{Corr}}^{\text{in}}}{R_{\text{Corr}}^{\text{un}}} \times 100, \quad (3)$$

$$\theta = \frac{\text{IE}\%}{100}. \quad (4)$$

Here, A is the total surface area in cm², t is the time of exposure in day, and $R_{\text{Corr}}^{\text{un}}$ and $R_{\text{Corr}}^{\text{in}}$ are the corrosion rates without and with the inhibitor, respectively.

All solutions were prepared using doubly distilled water and ethanol (99:1, vol:vol) and all electrochemical and gravimetric measurements were carried out in open to air (aerated) solutions at room temperature.

2.4 Raman spectroscopy

Raman spectra were measured using the microscope attachment of a J-Y T64000 Raman spectrometer operated in single spectrograph mode with a holographic dispersive grating of 600 grooves/mm, giving a resolution of 2 cm⁻¹. A 647.1 nm holographic notch filter was used to remove the Rayleigh-scattered light. The entrance slit width was 100 μm . A liquid nitrogen-cooled CCD was used to detect the scattered light.

3 Results and discussion

3.1 Open-circuit potential (OCP) measurements

The OCP curves of the copper electrode in aerated 3.5% NaCl in the absence (1) and presence of 0.5 (2), 1.0 (3), and 5.0 mM ATP (4) are shown in Fig. 1. It is clearly seen from the curve 1 that the chloride solution increased the potential to the more negative values in the first few minutes perhaps due to the dissolution of copper as can be represented by the following equation,

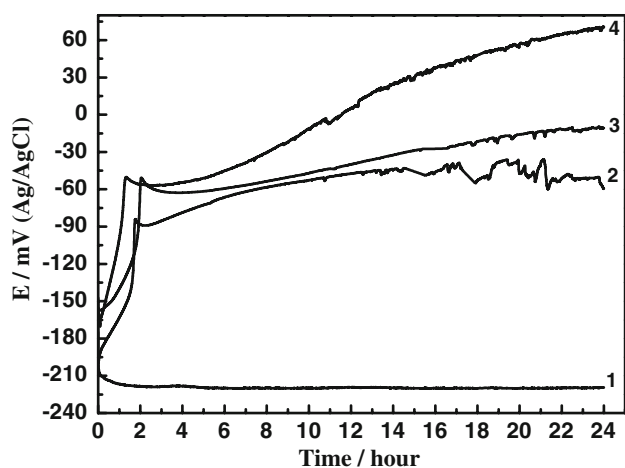


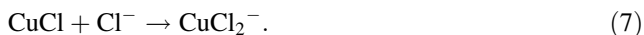
Fig. 1 Open-circuit potential versus time for copper in aerated 3.5% NaCl solutions without (1) and with 0.5 (2), 1.0 (3), and 5.0 (4) mM APT present, respectively



The resulting Cu^+ reacts with chloride ion from the solution to form CuCl [23],



The CuCl provides partial protection to the copper surface and transforms to the cuprous chloride complex, CuCl_2^- through which the dissolution of copper occurs and could lead to the slight negative shift in potential values with time [23, 24],



Under these conditions the corrosion of copper is under mixed control by the dissolution of copper and the diffusion of soluble CuCl_2^- from the Helmholtz plane into the bulk solution [25],



The presence of 0.5 mM APT (curve 2) abruptly shifts the OCP to less negative values from the first moment of copper immersion. This results from the adsorption of APT molecules onto the copper surface (see the Raman data) preventing the formation of cuprous chloride complexes and blocking the active sites on the copper surface. During the first 2 h (rapid stage) of immersion the OCP becomes substantially less negative attaining a value of -84 mV as a result of the stabilization of the APT film on the copper surface; thereafter the potential became less negative at a much reduced rate. Fluctuations started to appear on the curve after 15 h of the electrode immersion. Increasing the APT concentration to 1.0 (curve 3) and 5.0 mM (curve 4) showed essentially the same behavior with the OCP attaining values of -50 mV in the initial rapid stage but with no fluctuations with increasing time. It is concluded that the fluctuations in the OCP with the lowest

concentration of APT (0.5 mM) for extended time periods are indicative of corrosion occurring. Hence a sufficiently large concentration of APT is necessary to provide adequate surface protection.

3.2 Potentiodynamic polarization measurements

The potentiodynamic polarization curves of the copper electrode after 1 h (a) and 24 h (b) immersion in aerated 3.5% NaCl solution without (1) and with 0.5 (2), 1.0 (3), and 5.0 mM (4) ATP present, respectively are shown in Fig. 2. The cathodic reaction of copper in aerated NaCl solutions is well known to be the oxygen reduction [2, 4] namely,



The anodic dissolution of copper showed three distinct regions that have been reported in detail previously [1–4, 26]. In brief, these are; a Tafel region at lower overpotentials extending to the peak current density (j_{peak}) due to the dissolution of copper into Cu^+ , Eq. 5; a region of decreasing currents until a minimum (j_{min}) is reached due

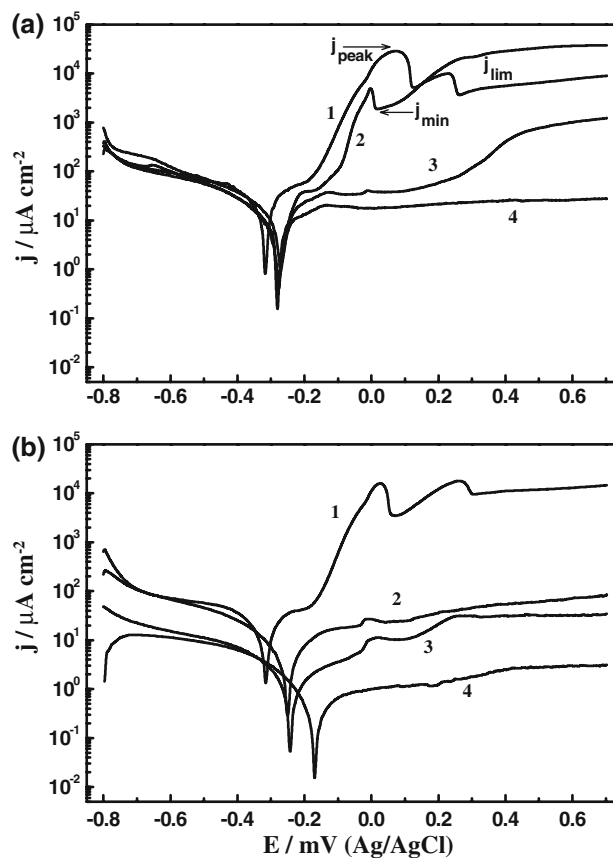


Fig. 2 Potentiodynamic polarization curves for copper in aerated 3.5% NaCl solutions after 1 h (a) and 24 h (b) of electrode immersion without (1) and with 0.5 (2), 1.0 (3), and 5.0 (4) mM APT present, respectively

Table 1 Corrosion parameters obtained from potentiodynamic polarization curves shown in Fig. 2 for copper electrode in aerated 3.5% NaCl solutions in absence and presence APT after different exposure times, 1 and 24 h

Solution	Parameter									
	E_{Corr} (mV)	j_{Corr} ($\mu\text{A cm}^{-2}$)	$-\beta_c$ (mV dec^{-1})	β_a (mV dec^{-1})	j_{peak} ($\mu\text{A cm}^{-2}$)	j_{min} ($\mu\text{A cm}^{-2}$)	R_p ($\text{k}\Omega \text{ cm}^2$)	R_{Corr} (mpy)	θ	IE (%)
3.5% NaCl only (1 h)	-317	19	140	125	29,000	5,400	1.51	8.71	-	-
0.5 mM APT (1 h)	-290	4.7	165	130	4,800	1,900	6.73	2.15	0.75	75.3
1.0 mM APT (1 h)	-280	2.5	172	170	40	35	14.87	1.15	0.87	86.8
5.0 mM APT (1 h)	-275	1.4	172	180	20	15	27.31	0.64	0.93	92.6
3.5% NaCl only (24 h)	-330	12	160	145	17,000	3,400	2.76	5.5	-	-
0.5 mM APT (24 h)	-260	1.6	170	180	35	25	23.76	0.73	0.87	86.7
1.0 mM APT (24 h)	-238	0.7	175	185	11	10	55.86	0.32	0.94	94.2
5.0 mM APT (24 h)	-162	0.15	176	190	1.3	1.1	264.8	0.07	0.99	98.8

to formation of CuCl , Eq. 6; and a region of sudden increase in current density leading to a limiting value (j_{lim}), as a result of CuCl_2^- formation, Eq. 7.

Addition of 0.5 mM ATP to both NaCl solutions after 1 and 24 h of electrode immersion (curves 2) significantly decreased the cathodic, anodic, and corrosion (j_{Corr}) currents, with the corrosion potential (E_{Corr}) values slightly shifted in the less negative direction; this effect is also more significant in 1.0 and 5.0 mM APT, especially after the 24 h immersion. It is immediately seen from Fig. 2 that the APT molecules substantially inhibit the anodic corrosion reactions more than the cathodic ones. The corrosion parameters such as E_{Corr} , j_{Corr} , cathodic (β_c) and anodic Tafel (β_a) slopes, j_{peak} , j_{min} , polarization resistance (R_p), corrosion rate (R_{Corr}), degree of surface coverage (θ), and the inhibition efficiency (IE%) obtained from Fig. 2 were calculated [6, 10] and listed in Table 1. It is seen that j_{Corr} , j_{peak} , j_{min} and R_{Corr} values decrease with slight positive shifts in E_{Corr} , while β_c , β_a , R_p , θ , and IE% increase in the presence of APT and the increase of its concentration. This indicates that APT precludes the dissolution of copper and provides its surface with more corrosion resistance by blocking its active sites and preventing the formation of chloride and oxychloride complexes.

3.3 Potentiostatic current–time measurements

In order to shed more light on the effect of APT on the anodic dissolution of copper and determine whether pitting corrosion takes place at more positive potential values, we carried out current–time experiments at 250 mV. Figure 3 depicts the measured current–time curves for the copper electrode after its immersion in the aerated 3.5% NaCl solutions without (1) and with 0.5 (2), 1.0 (3) and 5.0 (4) mM APT for 1 h (a) and 24 h (b), respectively. It is clearly seen from Fig. 3 that the highest currents are recorded for Cu in chloride solution in the absence of APT (curves 1).

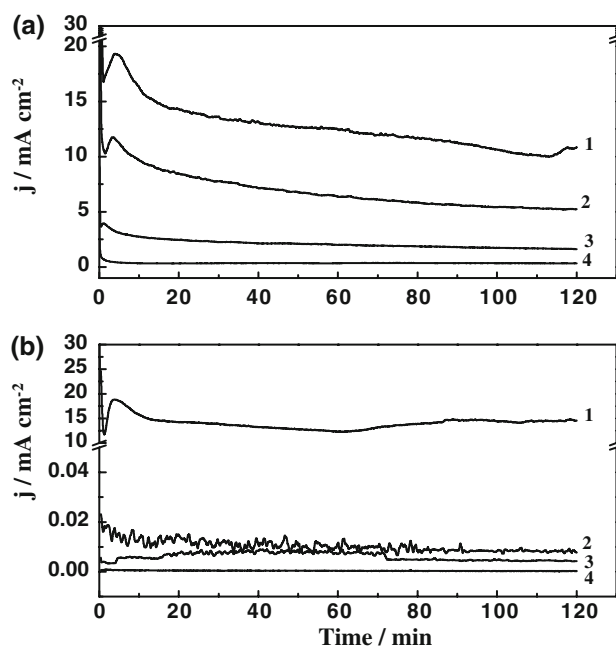


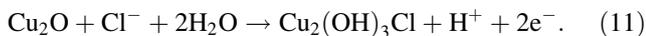
Fig. 3 Current–time curves recorded for copper electrode after its immersion in the aerated 3.5% NaCl solutions without (1) and with 0.5 (2), 1.0 (3), and 5.0 (4) mM APT present for 1 h (a) and 24 h (b); the applied potential was 250 mV versus Ag/AgCl for 120 min

This is due to the dissolution of copper by Cl^- ions and the formation of CuCl (Eq. 6), CuCl_2^- (Eq. 7) as indicated by the EDX analysis on the copper surface under similar conditions [4]. The decrease of current we see on curve 1 (Fig. 3a) is considered to result from the formation of a porous oxide layer (Cu_2O) according to the following reaction [3],



Furthermore increasing the immersion time of copper in the chloride solution to 24 h (Fig. 3b curve 1) leads to the

hydrolysis of the Cu₂O oxide layer resulting in an upper layer of atacamite (Cu₂(OH)₃Cl) [8],



The atacamite is neither protective nor compact enough to decrease the chloride ion attacks, leading to the current increases after ~65 min consistent with the occurrence of pitting corrosion seen with the naked eye after removing corrosion products from the copper surface.

The presence of 0.5 mM APT (curves 2) produces large decreases in the absolute current. This effect is even more significant with the increased immersion time of 24 h, where the current range over the whole experimental period was few microamperes. Increasing the concentration of APT to 1.0 and 5.0 mM APT (curves 3 and 4) recorded further small decreases of the respective currents with no indication of pitting corrosion. This agrees with the polarization measurements (Fig. 2) and confirms the ability of ATP molecules to inhibit pitting and general corrosion of the copper surface by preventing the formation of chloride and oxychloride complexes.

3.4 Electrochemical Impedance Spectroscopy (EIS) measurements

Figures 4 and 5 show respective Nyquist (a), Bode (b), and phase angle (c) plots obtained for copper in aerated 3.5% NaCl solutions without (1) and with 1.0 (2), 3.0 (3), and 5.0 (4) mM APT present, after 1 and 24 h immersion. In the presence of APT molecules the impedance spectra for the Nyquist plots after 1 h immersion (Fig. 4a) clearly show a small semicircle in the high frequency region followed by a straight line portion at low frequency values. The high frequency semicircle is attributed to the time constant of charge transfer and double-layer capacitance [27, 28]. The diameter of this semicircle grows with increasing concentration of the inhibitor as well as with the longer immersion time of 24 h (Fig. 5a); at this stage the charge-transfer resistance has become dominant in the corrosion process as a result of the formation of the protective APT film [29]. The segments for the lower frequency area in the absence of APT shown in the inserts (curves 1) are attributed to the diffusion of copper cations into the solution as indicated by Eq. 8. On the other hand and in the presence of APT, the increase of these low frequency segments is due to the adsorption then polymerization of APT molecules on copper followed by the formation of APT–Cu complexes on the electrode surface as follows,



The impedance spectra for the Nyquist plots (Figs. 4a and 5a) were analysed by fitting to the equivalent circuit model shown in Fig. 6. The parameters obtained by fitting the

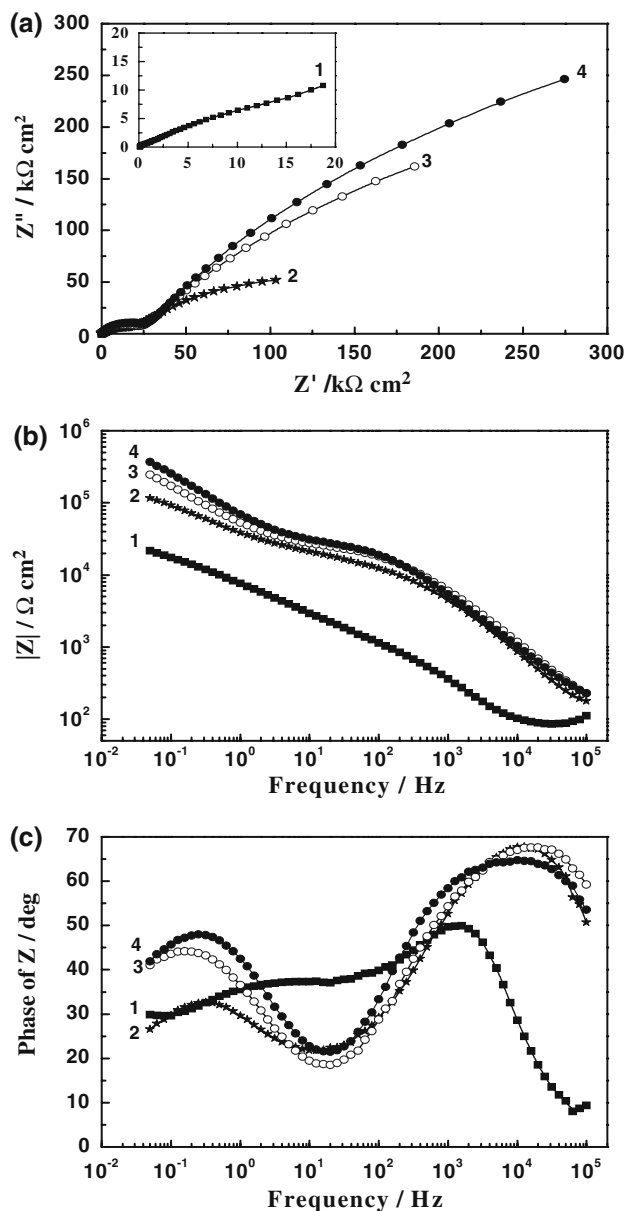


Fig. 4 Nyquist (a), Bode (b) and phase angle (c) plots for copper after 1 h immersion in 3.5% NaCl solution without (1) and with 0.5 (2), 1.0 (3), and 5.0 (4) mM APT present

equivalent circuit and the calculated inhibition efficiency are listed in Table 2. As can be seen from the equivalent circuit shown in Fig. 6, there are two routes for electron transfer, which are connected in parallel and competing with each other. Both of the routes are similarly affected by the presence of APT in the solution, and the difference between the two routes is currently not understood. The symbol R_s represents the solution resistance, R_p the polarization resistance, defined also as the charge transfer resistance, Q_1 and Q_2 are the constant phase elements (CPEs), and R_p^- another polarization resistance. It is seen from Figs. 4a and 5a and Table 2 that the R_s , R_p , and R_p^-

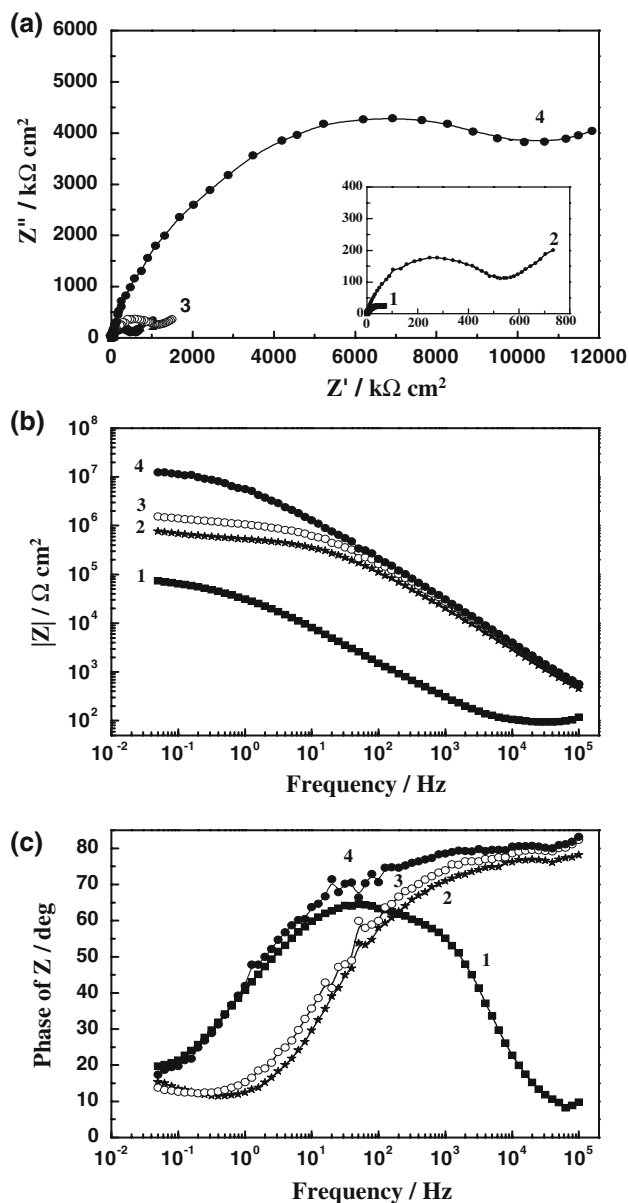


Fig. 5 Nyquist (a), Bode (b) and phase angle (c) plots for copper after 24 h immersion in 3.5% NaCl solution without (1) and with 0.5 (2), 1.0 (3), and 5.0 (4) mM APT present

values recorded for Cu in Cl⁻ solutions without the inhibitor increase as the immersion time increases, which agrees with the polarization data at the same condition and agrees with our previous work [8]. Also, the oxide layer covering the electrode surface in the absence of APT is fairly dense, although it is porous, as the CPEs have similar magnitudes Y_{Q_1} and characteristics typical of double-layer capacitances, their n values being 0.99 and 0.96 after Cu immersion for 1 and 24 h, respectively.

Addition of APT molecules raises the values of R_s , R_p , and R_p^- with further increases seen by increasing the APT concentration as well as the immersion time. The decrease

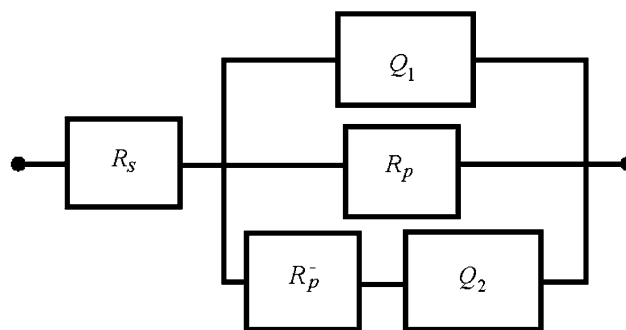


Fig. 6 An equivalent circuit used to fit the Nyquist plots shown in Figs. 4a and 5a. The symbol R_s represents the solution resistance, R_p the polarization resistance, Q_1 and Q_2 are the constant phase elements (CPEs), and R_p^- another polarization resistance

of CPEs, (Y_{Q_1}) values we have seen in Table 2 upon addition of APT and with increase in its concentration is due to the adsorption of APT molecules on the copper surface [30]. The CPEs, (Y_{Q_2}) appear to have Warburg characteristics with their n -values varying between 0.45 and 0.57 in all solutions suggesting that the mass transport may take place through the film. The IE% values of APT for the copper electrode were calculated from the charge transfer resistance as follows [3],

$$\text{IE}\% = [(R_p - R_p^-)/R_p] \times 100 \quad (13)$$

where, R_p , and R_p^- are the charge transfer resistances in the chloride solution with and without APT, respectively. Increasing the concentration of APT increases the impedance of the interface and the maximum phase angle as shown in Fig. 4b and c, respectively, which result from the inhibition of the corrosion processes. These effects increase with the immersion time as seen from Fig. 5b and c.

3.5 Gravimetric data, pH, inhibition efficiency and Raman spectroscopy

Figure 7 shows the variation of the dissolution rate (a) and pH (b) versus time for the copper coupons in 3.5% solutions without (1) and with 0.5 (2), 1.0 (3) and 5.0 mM (4) APT present, respectively. The dissolution rate and the pH increase rapidly with time in chloride solutions in absence of APT, being consistent with a high corrosion rate of copper. This is associated with the main species on the surface being CuCl_2^- , (Eq. 7) allowing the dissolution of copper via its diffusion into the bulk solution. The accompanying increase in pH also indicates that the rate of generation of OH⁻ ions by the cathodic reaction, Eq. 9, would be the same as that of CuCl_2^- ions. On the other hand, the presence of APT with increasing concentration greatly decreases both the dissolution rate and the corresponding pH values to a minimum even after the longest immersion time of 24 days.

Table 2 Parameters obtained by fitting the Nyquist plots shown in Figs. 4a and 5a with the equivalent circuit shown in Fig. 6 in 3.5% NaCl solutions in the absence and presence of APT

Solution	Parameter							IE (%)
	R_s (Ω cm ²)	Q_1		R_p (k Ω cm ²)	Q_2		R_p^- (k Ω cm ²)	
		Y_{Q_1} (μ F cm ⁻²)	n		Y_{Q_2} (μ F cm ⁻²)	n		
3.5% NaCl only (1 h)	44.2	5.76	0.99	4.64	4.4	0.48	0.28	–
0.5 mM APT (1 h)	54.5	0.198	0.81	52.67	1.23	0.51	13.5	91.2
1.0 mM APT (1 h)	72.4	0.177	0.83	85.4	0.71	0.53	24.7	94.6
5.0 mM APT (1 h)	96.5	0.13	0.79	93.8	0.45	0.56	30.1	95.1
3.5% NaCl only (24 h)	89.6	4.3	0.96	6.10	13.22	0.45	1.15	–
0.5 mM APT (24 h)	99.6	0.003	0.84	89.7	2.02	0.47	199	93.2
1.0 mM APT (24 h)	145.0	0.002	0.82	300	0.40	0.52	959	98.0
5.0 mM APT (24 h)	366.0	0.001	0.81	951	0.036	0.57	2,866	99.4

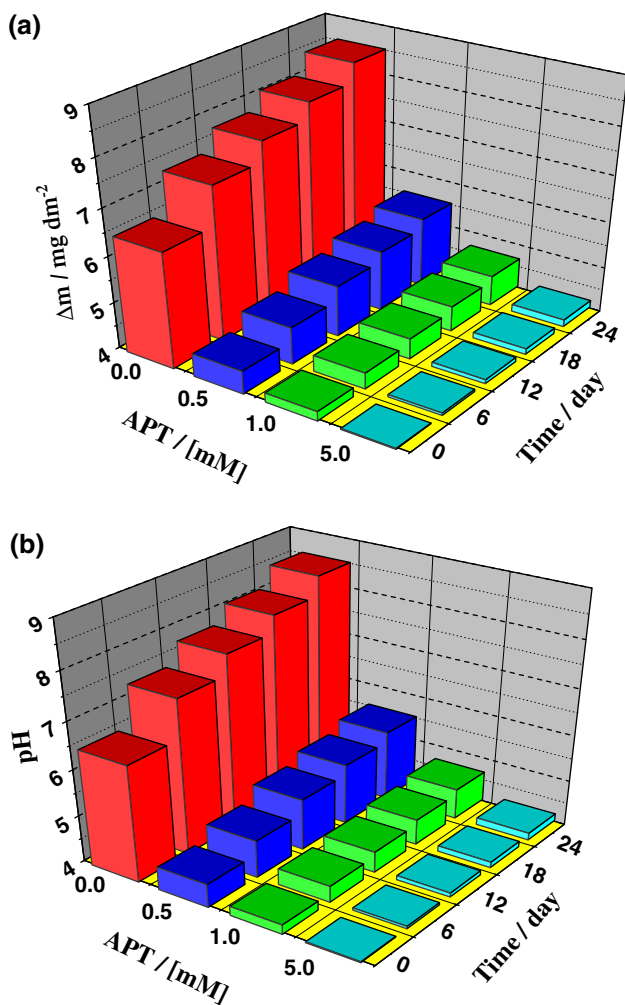


Fig. 7 Changes of the dissolution rate, Δm (a) and pH (b) with time for copper coupons in aerated solution of 3.5% NaCl solutions without (1) and with 0.5 (2), 1.0 (3), and 5.0 mM APT (4) present, respectively

Figure 8 shows the change of the percentage of the inhibition efficiency (IE%) versus time for copper in chloride solution containing 0.5 (1), 1.0 (2) and 5.0 mM (3)

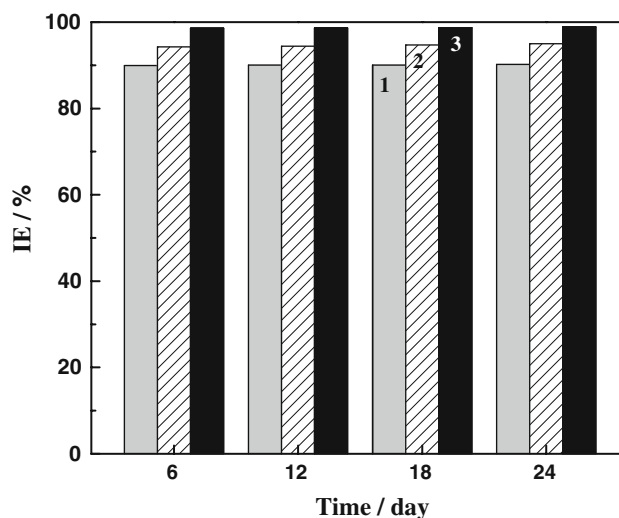


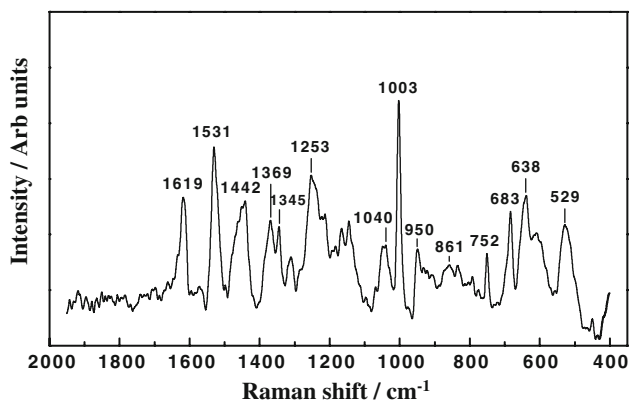
Fig. 8 Variation of the inhibition efficiency (IE%) versus time for copper coupons in aerated solutions of 3.5% NaCl in the presence of 0.5 (1), 1.0 (2), and 5.0 mM APT (3)

APT, respectively. The maximum IE% obtained for 0.5 mM APT was 90%, and increased to 95% and 99% when the concentration of APT was increased to 1.0 and 5.0 mM, respectively. It is noted that the IE% value remains essentially constant for each concentration of APT over the different periods of copper immersion. The values of the corrosion rate (R_{Corr}) and the degree of surface coverage (θ) using Eqs. 2 and 4 were also calculated, the data being shown in Table 3; increasing the APT concentration significantly raises θ and lowers R_{Corr} values due to the strong adsorption of APT molecules onto the copper surface.

The Raman spectrum obtained from the copper surface that was immersed in 3.5% NaCl containing 1.0 mM APT for 24 days is shown in Fig. 9. The majority of the Raman modes observed are characteristic of the presence of APT or its complex with copper in the film formed, namely:

Table 3 Change of the degree of surface coverage (θ) and the corrosion rate (R_{Corr}) obtained from weigh loss data for copper coupons in aerated 3.5% NaCl solutions in absence and presence of ATP

Time (days)	Parameter	Solution			
		3.5% NaCl (B)	+0.5 mM APT	+1.0 mM APT	+5.0 mM APT
6	θ	–	0.90	0.95	0.99
	R_{Corr} (mdd)	0.508	0.00498	0.00283	0.00071
12	θ	–	0.90	0.95	0.99
	R_{Corr} (mdd)	0.496	0.00494	0.00278	0.00068
18	θ	–	0.90	0.95	0.99
	R_{Corr} (mdd)	0.493	0.00491	0.00275	0.00066
24	θ	–	0.90	0.95	0.99
	R_{Corr} (mdd)	0.486	0.00488	0.00273	0.00064

**Fig. 9** Raman spectrum obtained on the copper surface after its immersion in 3.5% NaCl solution containing 5.0 mM APT for 24 days

529 cm^{-1} , azole ring torsion; 752 cm^{-1} , azole ring breathing; 861 cm^{-1} , Cu–N stretching vibration; 950 cm^{-1} , tetrazole ring; 1,003 cm^{-1} , intermolecular Cu–N stretching vibration due to interacting of APT^- anion with Cu(I); 1,040 cm^{-1} , –N=N– stretching; 1,253 cm^{-1} , CH in plane bending; 1,369 cm^{-1} , ring stretching due to N–H deformation; 1,442 cm^{-1} , 1,531 cm^{-1} , benzene ring stretching; 1,619 cm^{-1} , C=N– stretching [31–35]. The Raman results provide direct evidence of the adsorption of APT molecules onto the copper surface thus strongly supporting the model invoking the blocking its active sites and preventing it from being corroded easily.

4 Conclusions

The inhibition of corrosion processes on copper in aerated 3.5% NaCl by 5-(3-aminophenyl)-tetrazole (APT) has been studied and the results can be summarized as follows:

1. OCP, potentiodynamic polarization and potentiostatic current-time measurements indicated that APT considerably shifts the corrosion potential to more positive values and greatly decreases the cathodic, corrosion and

anodic dissolution currents. This effect was enhanced upon increasing both the immersion time of copper and APT concentration in the test electrolyte.

2. EIS experiments showed that APT molecules increase both the surface and polarization resistances of copper particularly after 24 h of immersion.
3. Gravimetric and pH measurements indicated that the dissolution rate of copper together with the solution pH values decrease remarkably as the concentration of APT increases. The values of IE% obtained from the weight-loss data were 90% at a concentration of 0.5 mM APT and increased to 95% and 99% when the APT concentration was increased to 1.0 and 5.0 mM, respectively. These IE% values remained essentially constant for each APT concentration over the different exposure times and even after 24 days of the copper immersion in the inhibited solution.
4. The Raman spectroscopic investigation confirmed that the inhibition of copper corrosion is achieved by strong adsorption of APT molecules on the copper surface.
5. The combined results indicate that APT is a powerful corrosion inhibitor for copper in aerated 3.5% NaCl solutions.

Acknowledgement The work carried out was supported by the DST/NRF Centre of Excellence in Strong Materials, who also awarded a Postdoctoral Fellowship to EMS.

References

1. El Warraky A, El Shayeb HA, Sherif EM (2004) *Anti-Corros Meth Mater* 51:52
2. Sherif EM, Park SM (2005) *J Electrochem Soc* 152:B428
3. Sherif EM, Park SM (2006) *Corros Sci* 48:4065
4. Sherif EM (2006) *J Appl Surf Sci* 252:8615
5. Sherif EM, Erasmus RM, Comins JD (2007) *J Colloid Interface Sci* 311:144
6. Sherif EM, Park SM (2006) *Electrochem Acta* 51:4665
7. Sherif EM, El Shamy AM, Ramla MM, El Nazhawy AOH (2007) *Mater Chem Phys* 102:231

8. Sherif EM, Erasmus RM, Comins JD (2007) *J Colloid Interface Sci* 309:470
9. Sherif EM, Park SM (2006) *Electrochem Acta* 51:6556
10. Sherif EM, Erasmus RM, Comins JD (2007) *J Colloid Interface Sci* 306:96
11. Sherif EM, Park SM (2005) *J Electrochem Soc* 152:B205
12. Sherif EM, Park SM (2006) *Electrochem Acta* 51:1313
13. Núñez L, Reguera E, Corvo F, Gonzalez F, Vazquez C (2005) *Corros Sci* 47:461
14. Zucchi F, TrabANELLI G, Fonsati M (1996) *Corros Sci* 38:2019
15. Zucchi F, TrabANELLI G, Monticelli C (1996) *Corros Sci* 38:147
16. Lakshminarayanan V, Kannan K, Rajagopalan SR (1994) *J Electroanal Chem* 364:79
17. Scendo M, Hepel M (2008) *J Electroanal Chem* 613:35
18. Ammeloot F, Fiaud C, Sutter EMM (1997) *Electrochem Acta* 42:4565
19. Sutter EMM, Ammeloot F, Pouet MJ, Fiaud C, Couffignal R (1999) *Corros Sci* 41:105
20. Elmorsi MA, Hassanein AM (1999) *Corros Sci* 41:2337
21. Al-Kharafi FM (1988) *Corros Sci* 28:163
22. Fontana MG, Staehle KW (1970) *Advances in corrosion science and technology*, vol 1. Plenum Press, New York
23. Yan CW, Lin HC, Cao CN (2000) *Electrochim Acta* 45:2815
24. Itagki M, Tagaki M, Wantanabe K (1996) *Corros Sci* 38:601
25. Bacarella L, Griess JC (1973) *J Electrochem Soc* 120:459
26. Lee HP, Nobe K (1986) *J Electrochem Soc* 133:2035
27. Barcia OE, Mattos OR, Pebere N, Tribollet B (1993) *J Electrochem Soc* 140:2825
28. Deslouis C, Tribollet B, Mengoli G, Musiani MM (1988) *J Appl Electrochem* 18:374
29. Amin MA (2006) *J Appl Electrochem* 36:215
30. Bentiss F, Lagrence M, Traisnel M, Hornez JC (1999) *Corros Sci* 41:789
31. Gardiner DJ, Gorvin AC, Gutteridge C, Jackson ARW, Raper AS (1985) *Corros Sci* 25:1019
32. Zawada K, Bukowska J, Calvo M, Jackowska K (2001) *Electrochim Acta* 46:2671
33. Thierry D, Leygraf C (1985) *J Electrochem Soc* 132:1009
34. Otieno-Alego V, Huynh N, Notoya T, Bottle SE, Schweinsberg DP (1999) *Corros Sci* 41:685
35. Villamil RFV, Corio P, Rubim JC, Agostinho SML (1999) *J Electroanal Chem* 472:112